

Integrated parametric multi-level information and numerical modelling of mechanised tunnelling projects

Jelena Ninić^{a,*}, Christian Koch^b, Andre Vonthron^c, Walid Tizani^d, and Markus König^e

^a Assistant Professor, Centre for Structural Engineering and Informatics, The University of Nottingham, Nottingham, NG7 2RD, United Kingdom;
Phone: +44-115-84-68933; E-mail: jelena.ninic@nottingham.ac.uk

^b Professor, Intelligent Technical Design, Bauhaus-Universität Weimar, Marienstraße 13a, 99423 Weimar, Germany;
Phone: +49-3643-58-4960; E-mail: c.koch@uni-weimar.de

^c Research Associate, Computing in Engineering, Ruhr-Universität Bochum, Universitätsstraße 150, 44801 Bochum, Germany;
Phone: +49-234-32-26174; E-mail: andre.vonthron@rub.de

^d Associate Professor, Centre for Structural Engineering and Informatics, The University of Nottingham, Nottingham, NG7 2RD, United Kingdom;
Phone: +44-115-951-3873; E-mail: walid.tizani@nottingham.ac.uk

^e Professor, Computing in Engineering, Ruhr-Universität Bochum, Universitätsstraße 150, 44801 Bochum, Germany;
Phone: +49-234-32-23047; E-mail: koenig@inf.bi.rub.de

* Corresponding author
Email address: jelena.ninic@nottingham.ac.uk (J. Ninić)

ABSTRACT

This paper presents a concept for parametric modelling of mechanized tunnelling within a state of the art design environment, as the basis for design assessments for different levels of details (LoDs). To this end, a parametric representation of each system component (soil with excavation, tunnel lining with grouting, Tunnel Boring Machine (TBM) and buildings) is developed in an information model for three LoDs (high, medium and low) and used for the automated generation of numerical models of the tunnel construction process and soil-structure interaction. The platform enables a flexible, user-friendly generation of the tunnel structure for arbitrary alignments based on predefined structural templates for each component, supporting the design process and at the same time providing an insight into the stability and safety of the design. This model, with selected optimal LoDs for each component, dependent on the objective of the analysis, is used for efficient design and process optimisation in mechanized tunnelling. Efficiency and accuracy are further demonstrated through an error-free exchange of information between Building Information Modelling (BIM) and the numerical simulation and with significantly reduced computational effort. The interoperability of the proposed multi-level framework is enabled through the use of an efficient multi-level representation context of the Industry Foundation Classes (IFC). The results reveal that this approach is a major step towards sensible modelling and numerical analysis of complex tunnelling project information at the early design stages.

KEYWORDS

Building Information Modelling; Industry Foundation Classes, mechanised tunnelling; multi-level modelling; numerical simulation; visualisation

1. INTRODUCTION

With increasing urbanisation and mobility, the need for underground tunnel facilities becomes evident. The efficient and safe design and construction of mechanised tunnels involves complex data management incorporating information not only about the tunnel structure, but also about the existing built infrastructure, the ground and the boring machine. In early design phases, crucial decisions have to be made, for example, on the alignment of the tunnel track in order to minimise the risks of settlement induced damage to existing buildings. This task can now be supported by sophisticated, process-oriented finite element (FE) analysis. However, the required FE models are characterised by a high degree of detail at high costs of preparation and computational effort preventing them from being readily applied during what-if scenario analyses at early design stages. The appraisal of different design alternatives is essential for ensuring optimal designs. Assessing the effects of various alternatives for tunnelling projects on the surrounding environment is a multi-disciplinary and complex problem. The current state of the art process is cumbersome and requires significant computing resources and time (sophisticated simulations including all details can take days or weeks to complete). This often leads to sub-optimal solutions which are not optimal in their effect on the existing infrastructure. However, at the conceptual phase, a designer often only needs approximate estimations for number of different scenarios, e.g. tunnel track alternatives. To ensure a seamless workflow, the computation time should be minimised. If preliminary analysis (with consideration of uncertainties) indicates potential hazards, a more detailed evaluation of the model is required.

BIM has gained increasing attention in complex infrastructure projects, simplifying the planning and analysis and increasing productivity in design and construction. In tunnelling applications, the BIM concept has been used to create a tunnel information modelling framework that creates and interlinks a ground model, a tunnel lining model, a tunnel boring machine model and a built environment model [1]. Furthermore, a multi-level information representation of the built environment has been developed to support planning and analysis tasks [2]. The use of Industry Foundation Classes (IFC) enables open data exchange between several BIM software and provides a high level of compatibility [3]. The IFC standard was originally developed for the modelling of buildings and has recently been [4] extended to other fields of application in civil engineering, including bridges [5], roads [6] and tunnels [1, 7]. Nevertheless, despite 20 years of continuous development and the fact that over 200 software tools are using IFC, the interoperability issues, such as data loss and misrepresentation, are still problematic in practical projects [3].

As the project dimensions in tunnelling projects significantly exceed those in building projects, the concept of multi-scale modelling using several level of details (LoDs) has been proposed [8, 2].

Borrmann et al. [8], for example, present a comprehensive concept for incorporating multi-scale representations with shield tunnel models to efficiently link BIM with Geographical Information Systems (GIS). Their approach uses spatial IFC elements for low LoD representations and physical IFC elements for the highest LoD representations. Very recently, Abualdenien and Bormann [9] have presented an approach to support the continuous refinement of a building from the conceptual to the detailed design stages using a multi-LOD meta-model. While the purpose of this meta-model is to ensure the consistency of both the geometric and the semantic information as well as the topological coherence across different LoDs within the information model, a link to a multi-LoD numerical model is not considered.

As opposed to the concept of level of development (LOD), or level of model definition (LOMD), that has been introduced by the American Institute of Architects (AIA) in collaboration with the American BIMForum [10, 11], this paper refers to level of detail, LoD. According to BIMForum (2013), LoD defines how much detail is included in the model element, whereas LOD defines the degree to which the element's geometry and semantic information have been thought through in the development process. LOD, in this sense, specifies the reliability and maturity of information in the model along the design process. In summary, this paper does not focus on the model development process, but on the degree of detail that is captured for both geometry (level of geometry – LOG) and semantic information (level of information – LOI) for each of the system components.

In current engineering practice, the proof of tunnel design is often carried out by employing numerical simulations [12, 13, 14]. These models are usually generated based on design documents and reports. Even if the underlying information needed for numerical analysis is stored in a BIM, the translation from an information model to a computational model is still dominated by manual work. Such an approach therefore incurs significant effort carried out by experts, and is furthermore susceptible to human error. Hence, it is evident that an automated link between information management (in the form of a BIM) and numerical analysis is necessary. Such a link will enable the continuous, error-free exchange of information between BIM and numerical simulation for the stages of design, construction, and operation of a project.

In the field of structural analysis, the link between information and numerical models has been recently addressed in [15, 16, 17, 18, 19] where FE methods and Isogeometric Analysis (IGA) are applied for the assessment of the structural behaviour. In tunnelling application, the first attempt of linking BIM and structural assessment by means of numerical modelling is presented in [20, 21, 22], where data obtained from a Tunnel Information Model (TIM) [23] is used for the automated

generation of a numerical model for a real-world tunnelling project, the Wehrhahn metro line in Dusseldorf.

Based on the above, it can be stated that there have been several successful attempts to (1) demonstrate the need of a multi-LoD information model, and (2) automate the link from an information model to a numerical model at one particular LoD. What is still missing is the link between, or integration of, a multi-LoD information model and a corresponding multi-LoD numerical model. As mentioned before, this link is required to ensure a seamless design-assessment workflow, with optimised modelling and computation time, for certain design stages. For this reason, this paper presents a concept for Simulations for multi-level Analysis of interactions in Tunnelling based on the Building Information Modelling technology “SATBIM”. This forms the basis for multi-level structural analysis of the settlement behaviour [24]. To this end, parametric representations for each of the system components (tunnel lining with grouting, soil with excavation, existing buildings, and tunnel boring machine (TBM)) are developed for three different Levels of Detail.

This parametric information model is then used to automatically generate numerical models to simulate the tunnel construction process taking into account appropriate LoDs per component and dependent on the current design objective. Finally, the integration of multiple LoD configurations into a single IFC file is implemented for each component to enable reusability of the model in the context of BIM. The proposed concept is implemented using Autodesk Revit and Dynamo, [25], and tested in a what-if scenario analysis for a small tunnelling project.

2. METHODOLOGY

2.1 Parametric multi-level modelling in urban tunnelling

The main idea of the SATBIM concept is to dynamically generate simulation models from a multi-level information model at the required LoD for the specific problem to be solved. For example, minimising the overall risk of damage to buildings induced by tunnelling needs high LoD for structures and topology of the soil, however for the lining structure and its installation process, a lower LoD is sufficient to achieve high accuracy of the solution (see Fig. 1, red arrows). For the assessment of the stability of the excavated soil, high LoD is required for the soil representation, medium for the lining structure, while the building can be represented at the low LoD, e.g. surcharge load (see Fig. 1, blue dotted arrows). On the other hand, estimating stresses in the tunnel structure needs low LoD for buildings and high LoD for lining and its installation process, while surface topology of the soil is not necessary for the accuracy of the results (see Fig. 1, black dashed arrows).

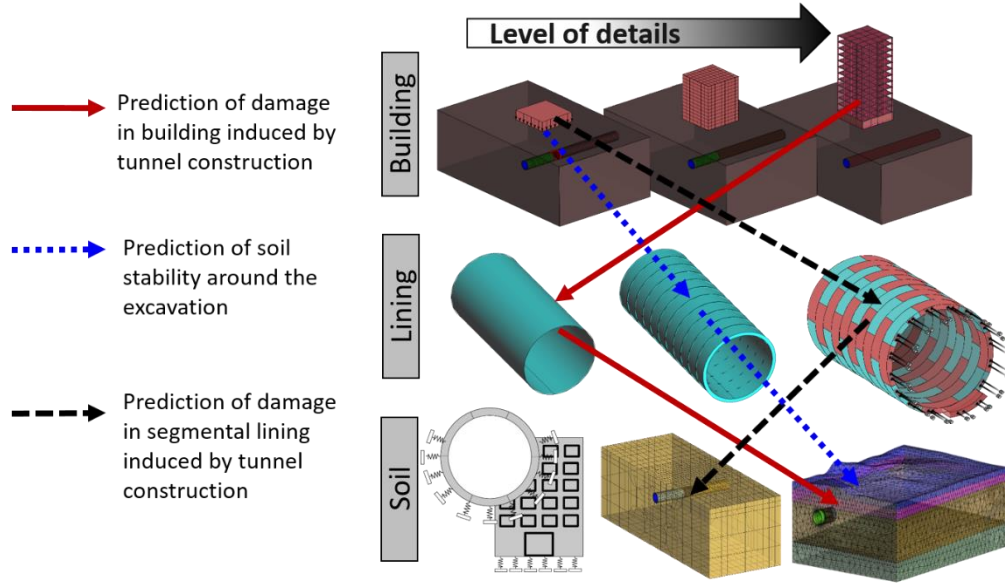


Figure 1: Alternatives for selection of LoDs for individual components based on the objective of the analysis

The shield-supported tunnel advance beneath groundwater table in soft soil requires permanent support of the surrounding underground to prevent the groundwater from flowing into the construction site. A realistic model to be applied during the design and construction phase has to represent all components of the tunnelling process relevant for the prognosis of the response of the surrounding soil during excavation. These components include:

- soil and excavation domain,
- segmental lining with the support measures applied at the tunnel face and at the tail void,
- tunnel boring machine (TBM), and
- existing infrastructure.

For each component three LoDs are defined: low (LoD 1), medium (LoD 2) and high (LoD 3). In general, the LoD 1 has no volumetric representation of the components, since in the corresponding numerical model, components are not represented with structural models but instead with the analytical or empirical models assigned through a set of boundary conditions. The medium LoD defines for each component a volumetric representation, where the component is “occupying” the exact volume; however the geometry is simplified. Finally, the highest LoD includes more detail about the actual geometry of the component. However, components such as TBM still do not include details of the machinery and the equipment inside the shield, and therefore, an even higher representation (LoD 4) could be introduced as an extension.

For each component and each LoD, a template of the corresponding component is defined. In order to keep consistency between different LoDs, parametric consistency is defined as shown in Fig. 2. The full set of parameters defining a component is needed for the definition of the highest LoD (LoD 3), while only a subset of the same list is used for the definitions of medium and lower LoD (LoD 2, LoD 1), respectively.

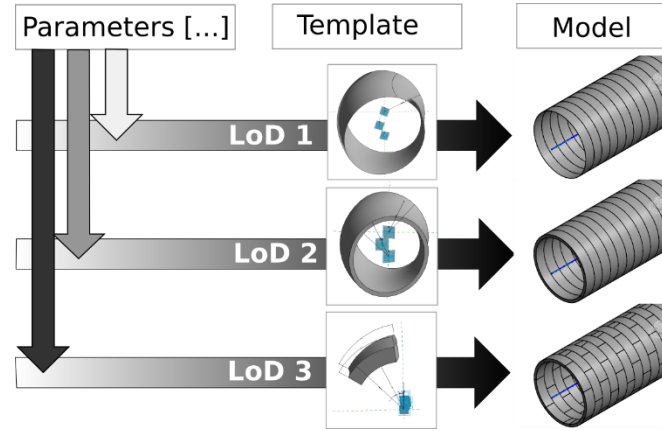


Figure 2: Parametric multi-level modelling: parametric consistency between different LoDs for individual components.

Combining all selected components at the selected LoDs (lining with its alignment and grouting, soil with excavation, TBM, and buildings), the complete tunnel information model is generated as shown in Figure 3. For each component, individual local parameters (LoD, geometrical and material parameters) are defined. On the other hand, there are also global parameters that are shared by multiple components such as ring length, excavation radius, number of steps/slices, overburden, etc. Further extensions for the multi-level representation of parametric components in the IFC format are presented in Section 2.6.

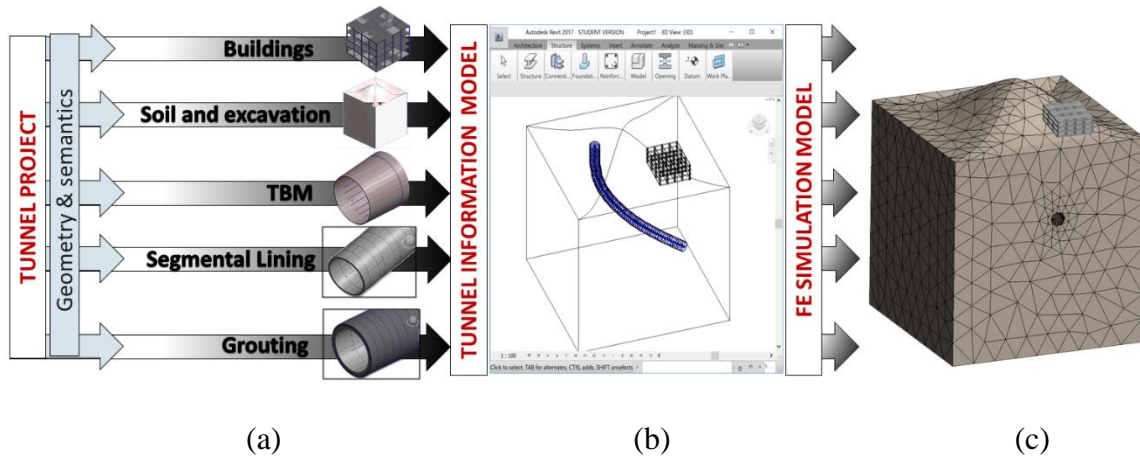


Figure 3: Multi-level tunnel information and numerical modelling. (a) Combining sub-models based on local and global parameters. (b) Integrated tunnel information model. (c) Generated numerical model

2.2 Modelling of the soil

Tunnelling projects are often characterised by complex geological conditions, where the construction is conducted through different, non-homogeneous geological layers under the ground water level. A ground model is developed based on ground investigations using boreholes and trial pits, commonly complemented by in situ testing and geophysical surveys, as appropriate to local needs and circumstances. Nowadays, tunnel project data including geotechnical information (geometry, topology, and attribute information such as groundwater data, associated geotechnical parameters, etc.) is stored either in 3D Geographic Information System (GIS) models [26, 27] or Geo Building Information Models (GeoBIM) [28]. GeoBIM has been developed to not only enable the management of subsurface construction, but also to support geo-related (subsurface) data, such as geological, hydro-geological and geotechnical objects and properties [28].

In numerical simulations of the mechanised tunnelling process, one of the most important requirements is the proper modelling of the soil behaviour, including complex hydraulic conditions. In relatively simple numerical models for the soil-structure interactions in tunnelling, the soil is represented by a set of boundary conditions. This is the case in the subgrade reaction model for the analysis of tunnel lining [29, 30] or the modelling of buildings with, for example, the Limiting Tensile Strain Method (LTSM) [31] or the Winkler beam method. For a more detailed representation of the tunnel construction with soil excavation, an explicit soil model with proper constitutive framework for the description of the hydraulic behaviour of the soil, as well as a realistic description of the material (stress-strain) response of the soil skeleton, is required.

2.2.1 Geometrical and numerical modelling

In terms of geometric and physical modelling of the soil, SATBIM approach offers all previously mentioned modelling variants, from simple representation of the soil with sets of boundary conditions to models considering multi-phase composition of the soil as well as accurate geometrical representation.

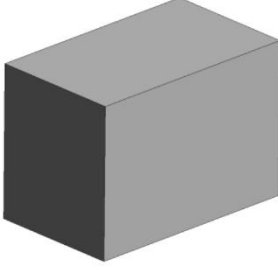
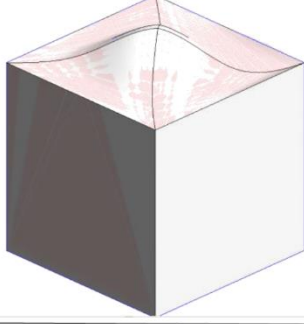
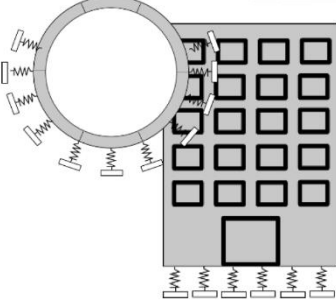
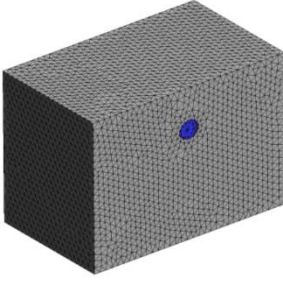
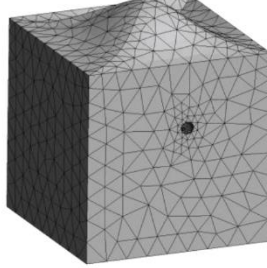
	LOD 1	LOD 2	LOD 3
Information model	<pre> 1 material soil_1 2 model_type drucker_prager 3 youngs_modulus 20000000.0 4 poisson_ratio 0.25 5 density 1732.0 6 porosity 0.4 7 cohesion 200000.0 8 hardening_modulus 2033333.0 9 internal_friction_angle 30.0 10 K0 1.0 11 permeability 1e-02 12 material soil_2 13 model_type drucker_prager 14 youngs_modulus 100000000.0 15 poisson_ratio 0.25 16 density 2038.0 17 porosity 0.25 18 cohesion 200000.0 19 hardening_modulus 50000000.0 20 internal_friction_angle 35.0 21 K0 1.0 22 permeability 1e-02 </pre>		
Numerical model			

Figure 4: Representation of the soil in information and numerical models on different LoDs.

Soil LoD 1. For the representation of the soil, a subgrade reaction model is adopted, where the soil is represented by infinitely thin, uncoupled springs neglecting the soil-structure interaction and the weight of the excavated soil (Fig. 4, LoD 1). The linear elastic subgrade reaction is obtained if the springs are linear ($p = K_s \cdot u$), where p is the pressure between the structure and the soil, K_s is the subgrade reaction modulus, and u is the deformation. The subgrade reaction approach permits the development of elegant analytical solutions for determining the deformation of buildings, using the Winkler equation:

$$EI \frac{\partial^4 w}{\partial x^4} = q_0(x) - r(x) \text{ where } r(x) = B \cdot K_h \cdot w(x) \quad (1)$$

where EI is the beam stiffness, B is the beam width, K_h is the coefficient of the horizontal subgrade reaction, while $w(x)$ and $q_0(x)$ are the deflection of the beam and load functions, respectively.

However, the challenge is to determine the subgrade reaction coefficient K_s , which cannot be measured directly. In a simple model proposed in [32] this coefficient is given as:

$$K_s = \frac{E_s}{B \cdot I_p (1 - \nu^2)} \quad (2)$$

where I_p is the shape factor of the foundation. When determining the subgrade reaction modulus of the springs for the lining model, according to [33], the stiffness of the spring is assumed to depend on the stiffness of the soil E_s , Poisson's ratio ν and the radius of the tunnel lining r :

$$K_s = \frac{E_s}{r} \frac{1-\nu}{(1+\nu)(1-2\nu)} \quad (3)$$

Soil LoD 2. In this LoD, the soil is represented by a structural finite element model, and the geometry, determined as a bounding box, is used to delimit the simulation model. The soil is modelled as a two-phase fully saturated material, accounting for the soil matrix and the pore water as distinct phases according to the theory of porous media (see [34, 35] for details).

Soil LoD 3. In terms of numerical modelling, the same FE representation of the soil (two-phase soil model for fully saturated soils) as for LoD 2 is employed here. However, the geometry is defined using the actual CAD geometry containing soil or rock layers, their boundaries, and their geotechnical properties in a standard format for tunnel ground models as shown in Figure 4. Therefore, for the representation of individual layers, distinct volumes are available, and hence distinct FE meshes are generated. In future extensions, interface conditions can be assigned between distinct soil layers to model interactions, sliding and redistribution of pore water pressures on the soil layer interfaces.

2.2.2 Material modelling

Besides establishing a proper constitutive framework for the description of the hydraulic behaviour of the soil, a key feature of a model for tunnelling is a realistic description of the material (stress-strain) response of the soil skeleton.

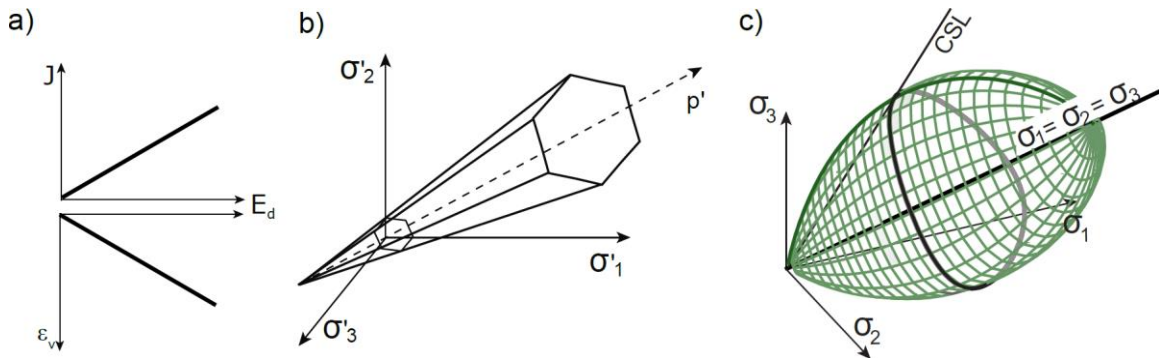


Figure 5: Examples for soil material models on different LoDs: a) LoD 1: Linear elastic model (Young modulus E , volumetric strain ε_v , deviatoric stress invariant J); b) LoD 2: Mohr Coulomb Model; c) LoD 3: Yield surface of CASM in principal stress state and in the p' - q plane [36].

Depending on the type of the soil and available material testing for model calibration, different material models can be applied. If there is no knowledge about the material behaviour, the simplest soil model which can be applied is a linear-elastic model (LoD 1). Since elastic behaviour is unrealistic for soils, different elasto-plastic constitutive models are available in KRATOS: the Mohr Coulomb and the Drucker Prager models, which are preferably used for sandy soils (LoD 2); and the more general Clay and Sand Model (CASM), characterised by non-associative plasticity and Lode-angle dependent yield surfaces [36], which is well suited for clayey soil (LoD 3) (see Figure 5).

2.3 Modelling of the segmental lining

The application of segmental lining as the final tunnel support and lining is a worldwide standard for shield tunnelling technology [37] as it fulfils the main construction requirements: i) to ensure the tunnel stability behind the shield; ii) enable short installation times and iii) provide abutment for the hydraulic jacks.

Each tunnel project has special lining requirements, depending on the diameter, soil conditions and alignment to guarantee a safe and durable tunnel structure for an expected lifetime of 100 years or more. In order to allow for a high modularity and efficient procedures for the production and logistics of the linings, the solution that is often adopted is to employ universal rings (see Fig. 6a). In most cases, the universal segment ring is made of several segments of the same size and of one smaller segment - the key-stone - closing the ring. The universal ring is characterised by an average ring length L_r , inner and outer radius of the ring (r_{inner} and r_{outer}), an angle describing the tapered geometry of the ring α , and the number of segments and their sequence within the ring.

2.3.1 Alignment

The designed alignment of the tunnel is accomplished by adjusting the rotations of the rings as shown in Fig 6a. For the curved parts, the rings are placed by lining up the key segments; for straight parts the rings are switched from upward key to downward key. The relative positioning of keys can be varied to modify the curved radius. The curvature of the alignment that can be achieved, given the geometry of the universal ring and the design theoretical alignment, is shown in Fig. 6b. Even though the final rotation of the ring will be determined dynamically during the tunnel construction to follow the TBM, in this paper, we developed an algorithm that determines these ring positions based on the initial design path. This is so to mimic reality and provide the best assessment of the design, taking into account the fact that ring rotations significantly affect the structural behaviour [38].

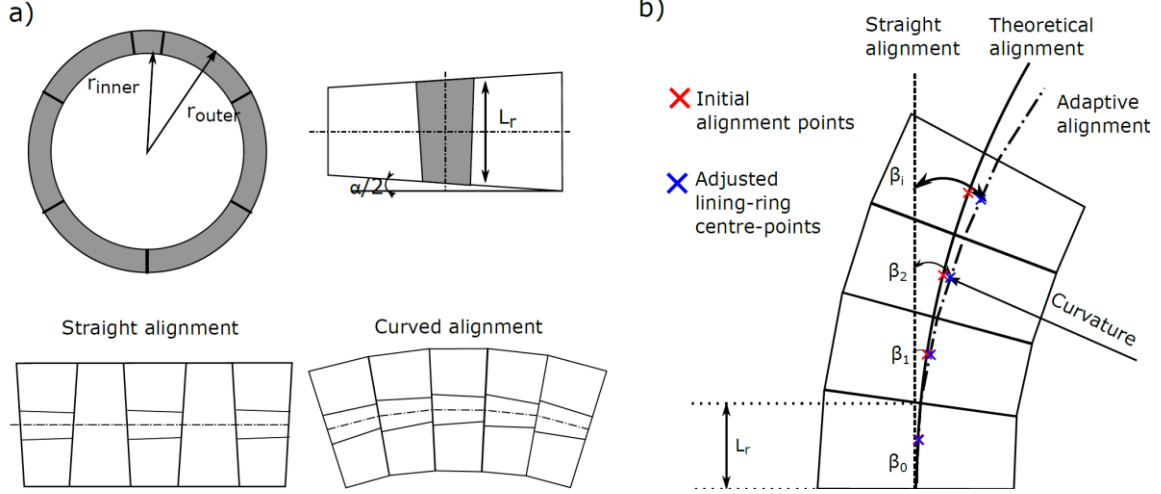


Figure 6: Forming the tunnel alignment based on the universal ring geometry: a) tapered geometry of universal ring (6+1); b) design alignment vs. adaptive alignment from appropriate rotations of ring segments

An algorithm for the calculation of the adaptive alignment has been developed. Based on the set of initial lining-ring centre-points and parameters L_r (ring length), α (ring continuity) and θ (rotation in ring plane), a new adjusted list of lining-ring centre-points is created by determining the rotation of the lining ring such that the centre-point of the adjusted lining-ring has minimal distance from the initial centre-points. As an output, a list of adjusted lining-ring centre-points (*list points*) and a list of locations of ring rotations in the plane normal to the alignment (*ring rotations*) are stored. The number of possible rotations in plane and, consequently, the angle $\Delta\theta$ depends on the number of segments and position of joints. There are alternatives in the ring installation strategy, such that, for instance, the next ring can be turned only for one $\Delta\theta$ clockwise or anti-clockwise, or alternatively it can be turned in any of possible rotation in the plane. Regardless of the ring rotation strategy, for any 3D design alignment, it is possible to determine the adjusted alignment following the geometrical transformation outlined below. Starting with an initial ring and its centreline coordinate x_{n-1} , y_{n-1} , z_{n-1} , and adding a new ring, we move to the new alignment point by a certain differential displacement

$$x_n = x_{n-1} + \Delta x_n \quad y_n = y_{n-1} + \Delta y_n \quad z_n = z_{n-1} + \Delta z_n \quad (4)$$

This differential displacement depends on the geometrical properties L_r and α , as well as the rotation θ of the ring in the ring plane as follows

$$\begin{aligned}
\Delta x_n &= L_r \cdot \cos \left(\beta_{n-1} + \frac{\alpha}{2} \cdot \cos(\theta_{n-1}) + \frac{\alpha}{2} \cdot \cos(\theta_n) \right) \\
&\quad \cdot \cos \left(\gamma_{n-1} + \frac{\alpha}{2} \cdot \sin(\theta_{n-1}) + \frac{\alpha}{2} \cdot \sin(\theta_n) \right), \\
\Delta y_n &= L_r \cdot \sin \left(\beta_{n-1} + \frac{\alpha}{2} \cdot \cos(\theta_{n-1}) + \frac{\alpha}{2} \cdot \cos(\theta_n) \right) \\
&\quad \cdot \cos \left(\gamma_{n-1} + \frac{\alpha}{2} \cdot \sin(\theta_{n-1}) + \frac{\alpha}{2} \cdot \sin(\theta_n) \right), \\
\Delta z_n &= L_r \cdot \cos \left(\beta_{n-1} + \frac{\alpha}{2} \cdot \cos(\theta_{n-1}) + \frac{\alpha}{2} \cdot \cos(\theta_n) \right) \\
&\quad \cdot \sin \left(\gamma_{n-1} + \frac{\alpha}{2} \cdot \sin(\theta_{n-1}) + \frac{\alpha}{2} \cdot \sin(\theta_n) \right)
\end{aligned} \tag{5}$$

We obtain the new inclination of the ring in the global coordinate system (in the XY plane β and the YZ plane γ) as

$$\begin{aligned}
\beta_{n+1} &= \beta_n + \frac{\alpha}{2} \cdot \cos(\theta_{n-1}) + \frac{\alpha}{2} \cdot \cos(\theta_n), \\
\gamma_{n+1} &= \gamma_n + \frac{\alpha}{2} \cdot \sin(\theta_{n-1}) + \frac{\alpha}{2} \cdot \sin(\theta_n)
\end{aligned} \tag{6}$$

The algorithm initialises the lining-ring centre-points of the design alignment, and searches for the rotation in the normal plane θ such that the deviation of the next centre point from the design path is minimised. Our implementation allows any tunnel path in 3D space to be achieved using only one universal ring. The agreement between the designed and the adapted tunnel alignment for one arbitrary case is shown in Figure 7.

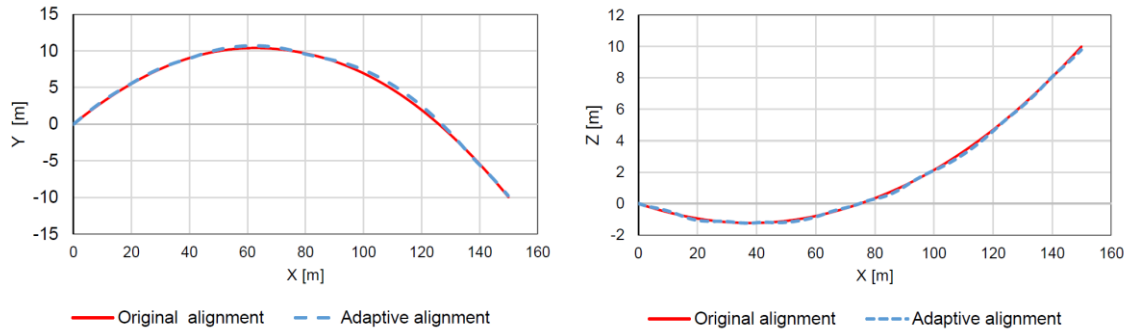


Figure 7: Comparison between designed alignment and computed adapted alignment based on universal ring in 3D in the a) XY plane, b) XZ plane.

A numerical analysis of the influence of the joints of the segmental lining on the overall behaviour of the tunnel structure is typically performed without consideration of the complete tunnel construction analysis, but rather by applying sophisticated models for lining and joints, and

observing the behaviour under design loads, while the resistance of the soil is modelled by subgrade reaction springs [29]. On the other hand, most sophisticated 3D simulation models for mechanised tunnelling do not consider the segment-wise installation of tunnel lining and joints between segments. Instead, lining is modelled using linear-elastic solid or shell elements, where the complete lining rings are installed stepwise [39, 40, 41]. Recently, a 3D numerical models for the shield tunnelling process was developed, where the influence of the joint pattern of the lining for both segment joints and ring joints is taken into consideration [13]. This study has shown that the position and stiffness of the joints have significant effects on the bending moment and normal forces in the lining, while the effect of the joint pattern on the surface settlement is insignificant. In the SATBIM concept, an alternative for modelling of tunnel lining is implemented, as described below, using the multi-level approach.

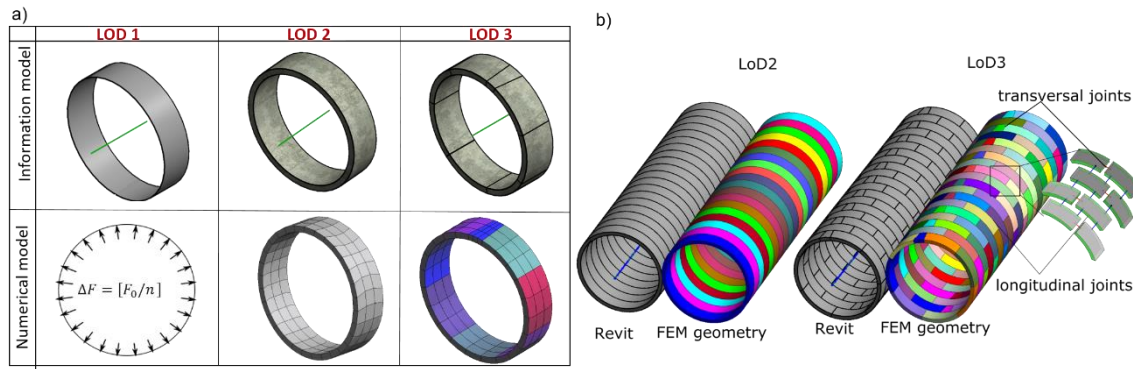


Figure 8: Lining information and numerical models on different LoDs, b) details of the geometry of the lining model on LoD 2 and LoD 3.

2.3.2 Geometrical modelling

Lining LoD 1. At the lowest LoD, the effect of the confinement and support provided by the lining structure on shield tunnelling is accounted for without explicit modelling of the lining structure. This is done by implementing the volume loss method, describing the confinement with the volume loss coefficient $V_l = \frac{(V_0 - V_{def})}{V_0}$. In this method, the volume loss resulting from the completion of excavation is prescribed together with the TBM passage (see Fig. 8a). The injection process and the grout consolidation phase are represented by applying the change in diameter of the excavation boundary. The method assumes that the support pressure at the tunnel boundary is reduced in increments, and the generated volume loss can be monitored.

In the implemented approach, the tunnel wall is allowed to move freely and is not controlled by confinement forces or prescribed displacements. Instead, after the de-confinement, the deformed

area of the tunnel is continuously calculated in each computation cycle during the displacement of the tunnel boundary. The deformations of the excavation boundaries are fixed when the volume loss value of the tunnel boundary is reached [42].

Lining LoD 2. The lining tube is modelled by means of volume elements that are activated during the simulated tunnel advance. Each lining ring is imported as a single volume, however, discretised by linear hexahedral finite elements (see Fig. 8 LoD 2). When simulating the tunnel advance, each lining ring is activated in a stress-free manner. This initialisation procedure is used to reset the reference configuration of the element. The new reference configuration of the re-activated element then matches the deformed state of the former structure.

Lining LoD 3. In order to account for the reduced stiffness of the tunnel lining due to the presence of joints and for the segment-wise installation of the tunnel lining, a model for longitudinal (ring) and transverse (segment) joints is proposed in the simulation model. Longitudinal and circumferential joints, are modelled in a discrete manner. The reduced stiffness of segmental lining ring due to the presence of joints is modelled by introducing bolts represented by beam elements and a surface-to-surface normal contact condition between segments and transversal joins of the lining rings, see Fig. 8b LoD 3. Bolts are embedded in the solid matrix representing the lining segments, where tying conditions are imposed between the integration points of the beam elements and control points in the solid segment elements with the same global coordinates. An additional normal contact condition between the facing surfaces of the segments in longitudinal and transverse direction prevents the penetration of one volume into another.

Grouting. The tail void grouting has a considerable effect on the changes of the initial stress state of the soil around the tail, which finally causes surface settlements. In particular, the re-distribution of the grouting mortar within the annular gap and the transition from liquid mortar, in the beginning, to solid state, after its hydration, plays a crucial role in maintaining the stress state of the surrounding soil and controlling the induced settlements. Therefore, in our simulation model, a constitutive model is applied that accounts for the time-dependent material behaviour of grouting mortar. Within the simulation model, the pressurization of the grouting mortar is accounted for using a two-phase formulation similar to the soil, as described in Section 2.2 for LoD 2/3. The hydration is described by time-dependent material properties for both the strength characteristics and the permeability. The formulation is based on the model for hydration of young concrete proposed in [43] and applied to grouting mortar in [44].

2.4 Modelling of the tunnel boring machine (TBM)

In shield tunnelling, the TBM is pushed forward by elongation of hydraulic jacks, and excavates the soil by a rotating cutting wheel and supports the material around the excavation area via the

shield skin. In terms of numerical modelling, there are different approaches of representing the shield machine. Since the main function of the shield is to prevent that the material around the excavation area moves into the tunnel excavation, one option is to represent the TBM simply by boundary conditions limiting the deformation of the soil [45]. However, the TBM is also a deformable body and the taper of the TBM and the frictional contact of the shield skin with its surroundings play an important role for the re-distribution of stresses and pore pressures in the soil. Therefore, the TBM can be represented using a 3D model interacting with the surrounding soil through a frictional interface [46]. An additional advanced modelling feature is to account for the hydraulic jacks that are attached to the TBM by using the previously erected lining segments as thrust bearings. In order to prevent divergence of the machine from the alignment, the thrust jacks are also used to steer the shield by setting different jack pressures [18].

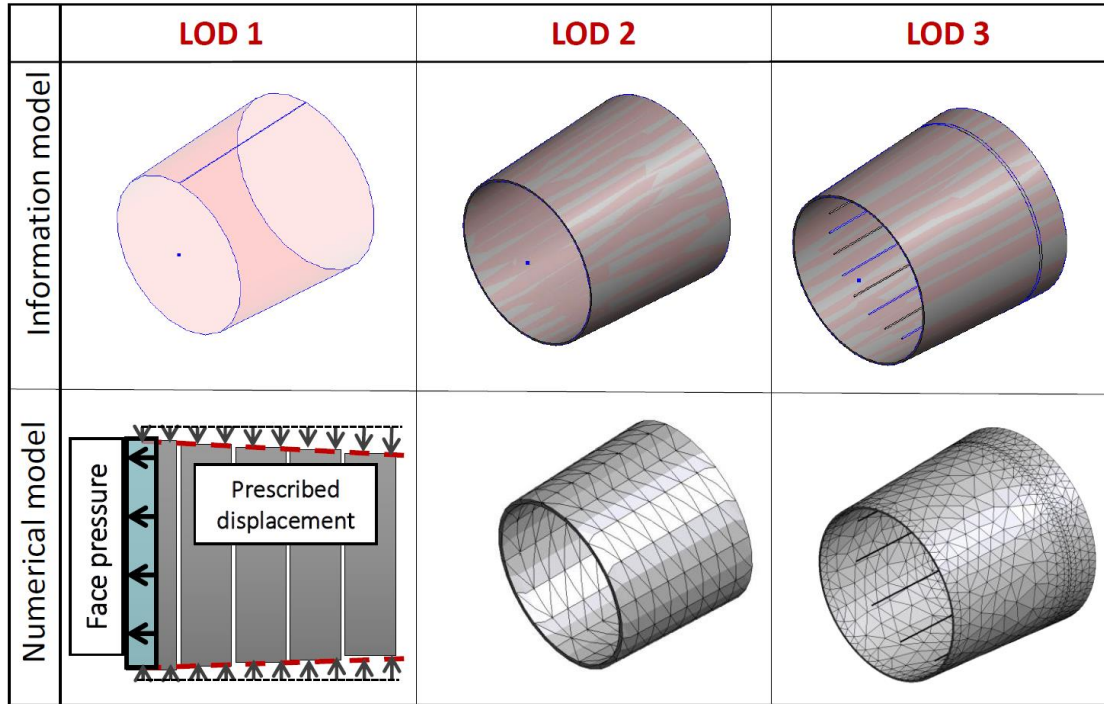


Figure 9: Information and numerical modelling of the TBM on different LoDs.

TBM LoD 1. To model the TBM as an obstacle for limiting the deformation of the soil, the shield is represented by boundary conditions [45], as illustrated in Figure 9. In this approach, the shield is represented by a set of n segments with length L_r with uniformly defined boundaries in terms of radial displacements that approximate the conical surface of the shield, where $n = L_{TBM} / L_r$ and L_{TBM} is the total length of the machine.

TBM LoD 2. The TBM is modelled as a deformable body moving through the soil and interacting with the ground using surface-to-surface contact. By virtue of this modelling approach, the volume

loss due to the excavation process naturally follows the real, tapered geometry and the over-cutting of the shield machine [40]. The frictional contact between the shield skin with the surroundings plays an important role in the re-distribution of stresses and pore pressures in the soil. It is therefore modelled by means of surface-to-surface contact formulation introduced by [47]. The contact formulation imposes a geometric constraint between the contacting (“slave”) body (the TBM) and the contacted (“master”) body (the soil) which controls the interaction between the two bodies with independent deformations. The displacements of the TBM are prescribed at the TBM tail, and the direction of advance is determined by the calculated tunnel alignment vector.

TBM LoD 3. The highest LoD describes the advancement of the TBM by elongation of hydraulic jacks, excavating the soil with a rotating cutting wheel. In order to realistically model the movement of the TBM and its interaction with the soil, to avoid drift off-course of the TBM and to simulate curved tunnel advances, an automatic steering algorithm, to control the individual jack thrusts similar to the one proposed in [44], is used to keep the TBM on the designed alignment path (see [18] for details). Identical to LoD 2, the interaction between the soil and TBM skin is modelled by applying frictional surface-to-surface contact conditions.

2.5 Modelling of the existing infrastructure

Tunnelling-induced settlements in urban areas are influenced by the interaction of existing structures (e.g. buildings) with the soil deformations. To consider this mutual influence, reduced models for structures are generally sufficient. However, if the objective of the analysis is to assess the effect of tunnelling on the behaviour of existing structures, detailed structural models are required. The selected LoDs for the representation of buildings are chosen such that the lowest LoD will not introduce any additional DoFs, but represent the buildings by means of additional stresses due to building weight, while the higher LoDs have a detailed representation of the building structure and include the relevant soil-structure interaction effects (see Figure 10). In the current state of development, a liner elastic material model is used for building representation, which can be used for damage detection using model updating techniques [48]. For direct estimation of a damage index, non-linear damage models are to be developed in future extensions of the framework.

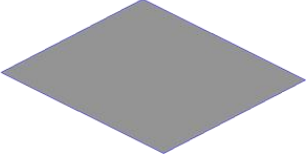
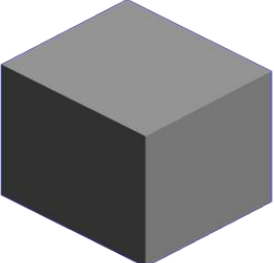
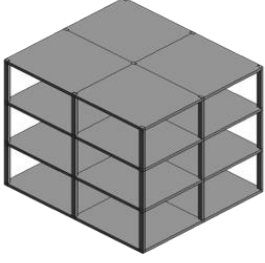
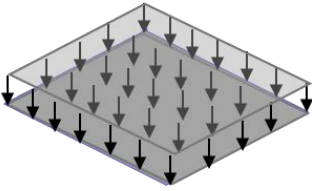
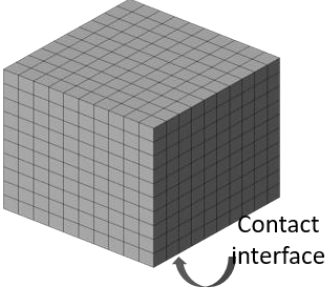
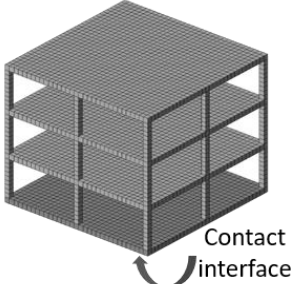
	LOD 1	LOD 2	LOD 3
Information model			
Numerical model			

Figure 10: Information and numerical modelling of existing buildings using different LoDs

Building LoD 1. The building is substituted by a dead load from the building weight acting on the soil surface as shown in Figure 10 (LoD 1). In this model, the effect of the soil-structure interaction and building stiffness are neglected. An algorithm is implemented to search the nodes in the soil domain that corresponds to the polygon of the building footprint. A distributed building dead load is applied to this group of nodes.

Building LoD 2. Buildings are considered in the tunnelling model by means of reduced models with a substitute elastic stiffness E , height H and weight, computed according to an approach proposed in [49]. In the presented FE formulation, isotropic volume tri-linear hexahedra elements are adopted with respective structural properties, interacting with the soil through a mesh-independent surface-to-surface contact algorithm, which prevents the penetration of the foundation of the building into the soil. It also takes into account the different mechanisms of the soil-structure interaction corresponding to the “sagging” and “hogging” modes.

Building LoD 3. Buildings are modelled as full structural frame models. The columns and floors are both modelled with isotropic volume hexahedra elements. In order to control the number of DoF, a quadratic structured mesh is generated, where a user-defined parameter is assigned to control the mesh size. For a detailed assessment of the stresses induced in the structures, the appropriate mesh size should be determined based on convergence studies. Since foundations

play a fundamental role in the transmission of the ground deformations to the building, surface-to-surface contact conditions are introduced between the soil and foundation to simulate such relative deformations,.

2.6 Multi-level information modelling in IFC

The Industry Foundation Classes (IFC) are considered as an appropriate information exchange format to support several BIM use cases throughout the facilities life-cycle, such as high-fidelity one-way design transfer, design coordination and checking among different disciplines, facility management handover, facility inspection and maintenance as well as visualisation [50]. For this reason, it makes sense to come up with a concept for representing multi-LoD information models in IFC to eventually be able to support these use cases.

Generally, there are two different approaches for representing geometry at different levels of detail in the Industry Foundation Classes (IFC). The first approach employs several separate IFC files for each level of detail. The second approach focuses on using different representation contexts to distinguish different levels of detail within one IFC File. Figure 11 outlines a class diagram that shows how to use such contexts. By concept, each *IfcProduct*, which includes geometrical representation, assigns an *IfcProductRepresentation*. Usually, this product representation includes exactly one *IfcRepresentation*, which defines one shape model. The actual geometric information is then assigned using one or multiple instances of *IfcRepresentationItem*. It also assigns a default *IfcGeometricRepresentationContext* that provides information about dimension, precision, coordinate system and true north. It further allows the assignment of multiple instances of *IfcGeometricRepresentationSubContext* “... to define semantically distinguished representation types for different information content ... to control the level of detail of the shape representation that is most applicable to this geometric representation context.” [43].

Comparing these approaches, there are advantages and limitations to each. Using separate files for representing different levels of detail does not depend on the format itself. Also, it does not require target software to support different representation contexts, but it requires the user to maintain an appropriate naming structure outside the file format and loading different level of detail manually into the target software. When considering not only geometric content, but also different sets of properties, which are assigned to separate levels of detail, using different files is error-prone.

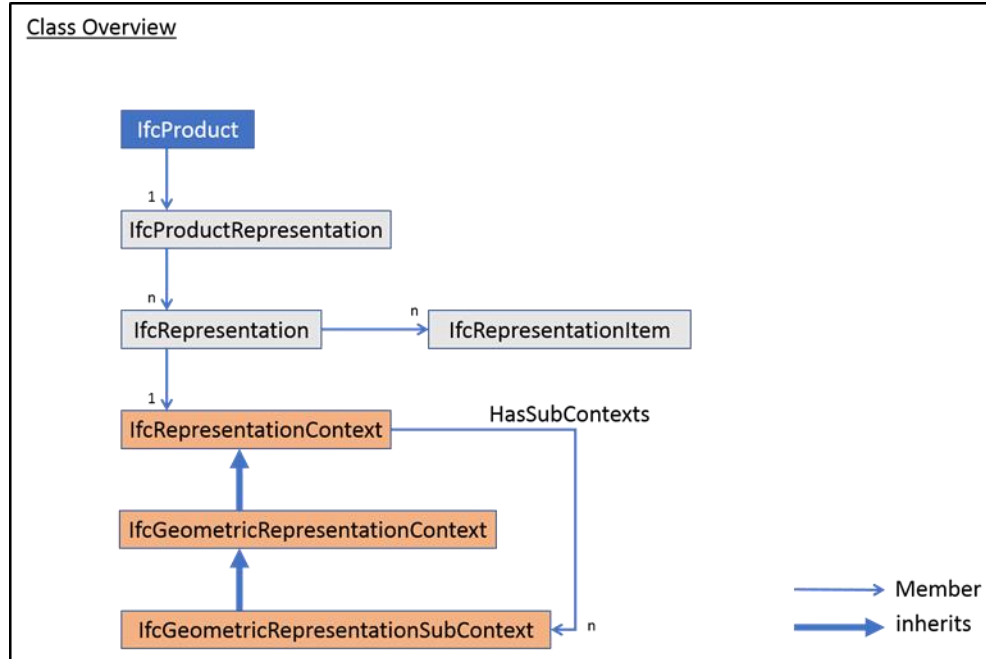


Figure 11: UML Class Diagram of IfcRepresentationContext

Using the IFC built-in concept of the *IfcRepresentationContext*, a proper decoupling between semantic and geometry levels of detail can be implemented by concept but requires the target software to support such contexts. This approach also allows the storing of all possible levels for each product. However, in this case the modeller should account for not overloading the IFC content by unnecessary levels of detail that may result in performance issues. Furthermore, this approach only applies for the geometric content, whereas the different sets of properties cannot be bound to a specific context. A workaround could store different sets for each level of detail, which, for example, can be linked afterwards by using the *IfcGeometricRepresentationContext*'s value of the attribute *UserDefinedTargetView*, like "LoD1", as an identifying prefix.

3. IMPLEMENTATION AND CASE STUDIES

3.1 Prototype implementation

The multi-level information model for tunnelling is developed using the industry-standard tools Revit and Dynamo [25], allowing for consistent parametric modelling on different LoDs. For each tunnel component and for each LoD, a template for the corresponding component is created using "Revit families". A family in Revit is a class with parametric definitions and constraints, allowing the definition of specific family attributes for individual family instances (Revit objects). In order to keep consistency between different LoDs, A parametric consistency between templates is defined in SATBIM as shown in Figure 2 and as introduced in Sections 2.2, 2.3, 2.4, and 2.5. The full set of parameters defining a component is needed for the definition on the highest LoD, while

only a subset of the parameter list is used for lower LoDs. This way of handling parameters allows for automated preservation of the consistency of the multi-scale model.

For each model component for each LoD, a corresponding numerical model has been developed using the pre/post processor GiD [51] and the open source Finite Element simulation software KRATOS [52]. The generation of the complete structural model, consistency between individual components, simulation scripts and visualisation features are handled by our newly developed software called “SatBimModeller”. A Python routine, *MaterialPropertiesUtility*, is used to enable a user-friendly input of the material properties. All details about the newly developed modeller can be found in [53]. The validation of the proposed computational framework can be found in [20, 21].

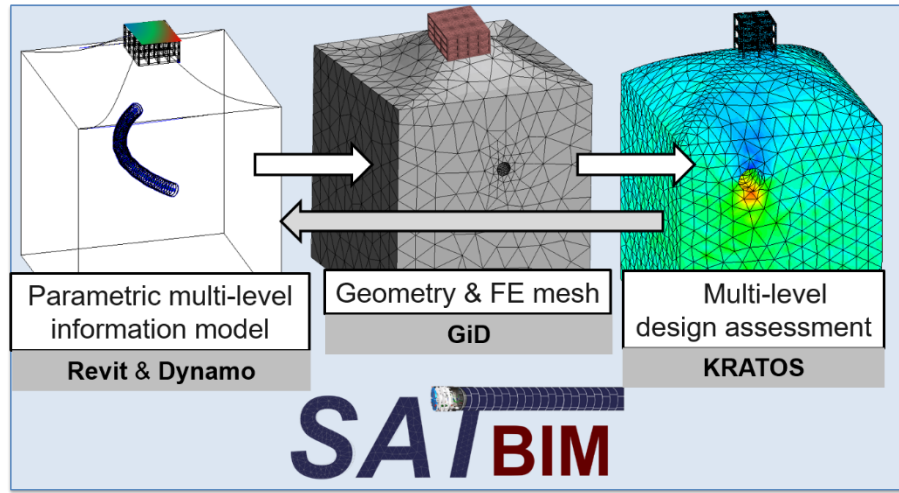


Figure 12: Workflow and implementation of the SATBIM framework

3.2 LoD selection for different scenarios of the analysis

The choice of the component LoD in both information and numerical model depends on the scenario of the analysis and the maturity of the analysis (in earlier design stages only approximate or relative quantities are sufficient). Higher accuracy in modelling leads to more reliable design assessment. However, this will also incur high modelling and computational costs. Therefore, an optimal LoD should be selected depending on the objective of the analysis and information available at the current stage of design. The following examples will discuss different scenarios for the selection of LoDs for the analysis of tunnelling-induced settlements and deformation of the structure.

The first problem exemplifies the selection of the building LoD for the estimation of tunnelling-induced settlements. In the example shown in Figure 13, a building with dimensions $18.5\text{ m} \times$

12.5 m × 15.8 m (length × width × height) is located above a tunnel of 10 m diameter (D). The middle axis of the building is offset from the centreline of the tunnel by 10 m (1D), and the tunnelling-induced settlements trough is observed for a building representation at LoDs 1-3 (accounting for building weight), soil at LoD 2, lining at LoD 1 (the volume loss method, with $V_l = 0.5\%$) and the TBM at LoD 1. The plot in Figure 13 shows the importance of the choice of the building LoD for both settlements and structural deformation. Maximum settlements are obtained for building LoD 1 due to the negligence of the building stiffness in soil-structure interaction. In contrast, for building LoD 2, this interaction effect is overestimated (very stiff structural response), compared to LoD 3, where a balance between soil and building stiffness is achieved.

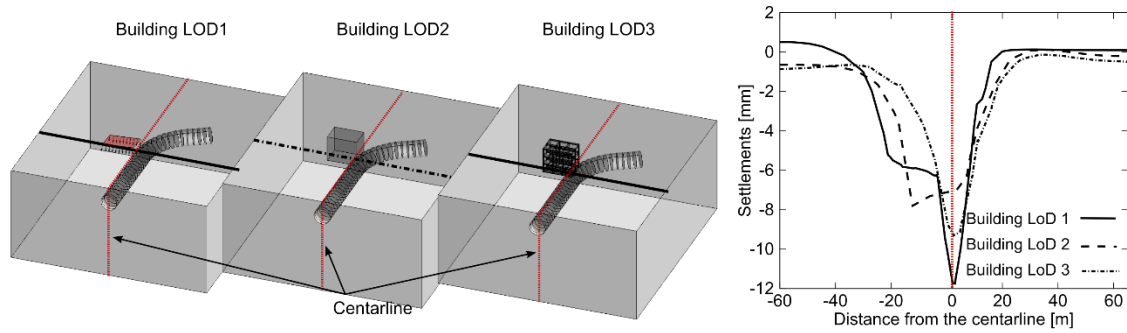


Figure 13: Impact of building LoD representation on tunnelling-induced settlements when the building is above the tunnel

In contrast, if the building is located far from the tunnel (middle axis of the building is offset from the centreline of the tunnel by 50 m (5D)), as shown in Figure 14, the choice of the building LoD is irrelevant, since tunnelling-induced settlements do not depend on the building representation. A detailed analysis of the sensitivity of building LoD representation to the building distance from the tunnel alignment and the tunnel depth can be found in [54]. These analyses show that the LoD of the building is irrelevant if the distance of the building from the tunnel centreline is larger than 4D.

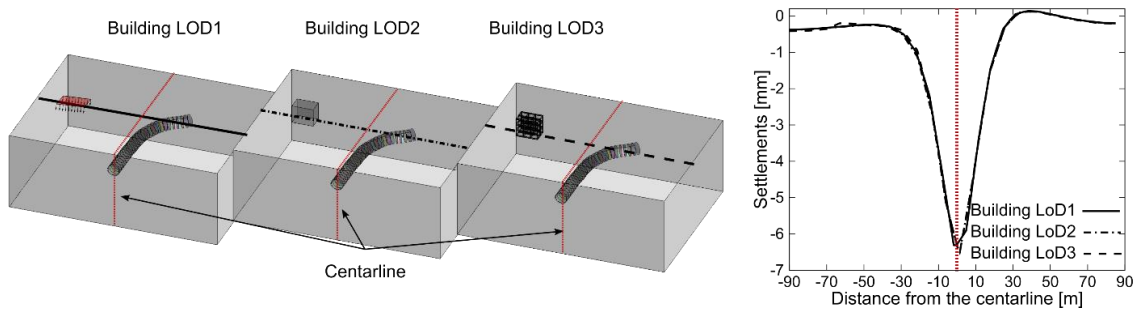


Figure 14: Impact of building LoD representation on tunnelling induced settlements when the building is far away from the tunnel

The second scenario investigates the effect of the selection of the soil LoD on the tunnelling-induced settlements and the deformation of the tunnel structure. In this example, lining and TBM are modelled at LoD 2, while the soil material is varied from LoD 1 (Linear Elastic model - LE), LoD 2 (Mohr Coulomb - MC) to LoD 3 (CASM) with the properties given in Table 1. From the plot shown in Figure 15, it is clear that introducing the non-linearity in soil behaviour, i.e. higher LoD, results in higher settlements. From the illustrated deformed tunnel ring, on the right side of Figure 15, it can be seen that higher settlements will cause higher vertical movement of the ring. However, the difference in ring shape is very small, because the ring moves almost as a rigid body. Therefore, the induced structural forces in all three cases are similar. Hence, if the target of analysis is the estimation of soil stability, then a higher LoD for the soil should be selected, however, the lining can be modelled at LoD 2.

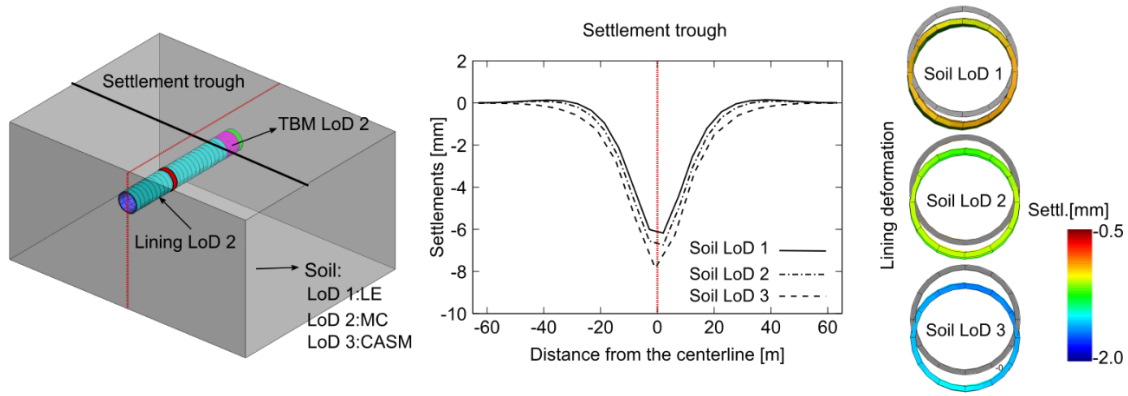


Figure 15: Tunnelling-induced surface settlements trough and lining ring deformation for soil representation using LoD 1: LE, LoD 2: MC, and LoD 3: CASM

Table 1: Material parameters for the soil models for examples in Figures 14, 15, 16

Component	Soil			Lining	TBM
Constitutive law	LE	MC	CAS	LE	LE
Young modulus (MPa)	80	80	80	2×10^4	2×10^5
Poisson ratio	0.25	0.25	0.25	0.3	0.3
Density (kg/m ³)	1732	1732	1732	2500	7620
Porosity	0.4	0.4	0.4	—	—
Cohesion (kPa)	—	200	—	—	—
Hardening modulus (MPa)	—	58.3	—	—	—
Friction angle (degrees)	—	30	—	—	—
Dilatancy angle (degrees)	—	30	—	—	—
Permeability (m/s)	0.00	0.00	0.001	—	—
Slope of the unload/reload curve in $(v - \ln p')$ space, κ	—	—	0.001	—	—
Slope of the normal compression curve in $(v - \ln p')$ space, λ	—	—	0.01	—	—

Spacing ratio, r	—	—	0.2	—	—
Shape parameter of the yield surface, n	—	—	2	—	—
Slope of the critical state line under triaxial compression, M	—	—	1.08	—	—
Initial preconsolidation mean stress for soil, P_0 (kN/m ²)	—	—	10^{15}	—	—

The third scenario, shown in Figure 16, investigates modelling of the tunnel lining, where the same model as in scenario 2 is used in terms of geometry and modelling of TBM. The soil is modelled at LoD 3, and the tunnel lining is modelled either using the volume loss method (LoD 1), as a solid ring (LoD 2), or as a segmented ring (LoD 3). For the volume loss method (lining LoD 1), we need to predefine the volume loss coefficient, which for this example $V_l = 0.8\%$ is used. This resulted in a slightly different settlements trough for lining LoD 1 (0.3 mm) compared to lining LoD 2 and LoD 3, which are almost identical (see Figure 16 settlement trough). However, if the deformation of the lining ring for LoD 2 and LoD 3 are compared, we can see, as seen in scenario 2, that the solid ring moves vertically as a rigid body, while the segmented ring deforms to a more oval shape, which will induce higher forces. Hence, for the estimation of surface settlements lining LoD 2 is sufficient, however, if one needs detailed insight into the structural deformation, lining LoD 3 is required.

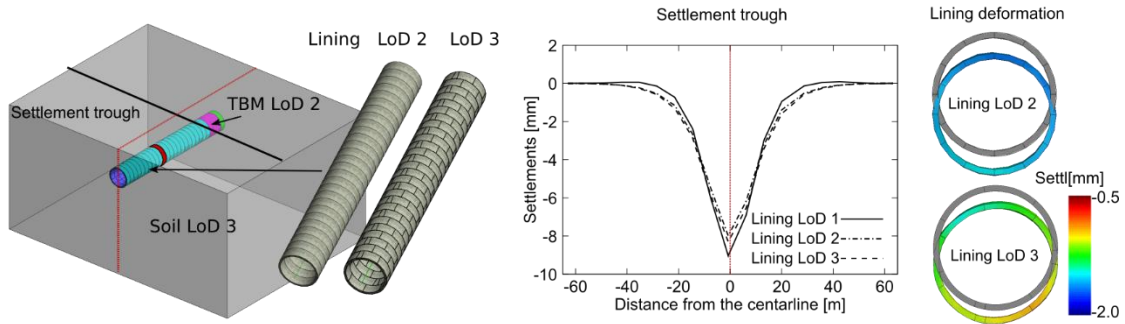


Figure 16: Impact of lining LoD on the tunnelling-induced surface settlements trough and the lining ring deformation

For further details about model sizes, FE meshing and simulations setup, all models are available in the SATBIM repository at <https://github.com/satbim/satbim/>.

3.3 Multi-level simulation of a tunnelling project

The SATBIM platform has been successfully applied for the generation of information and numerical models and for the visualisation of structural assessment. Depending on the design scenario, the optimal LoD of each individual component is selected, leading to a robust and computationally efficient numerical assessment (see Figure 17). Knowledge about the optimal building LoD for the scenario of shield tunnelling in the vicinity of existing infrastructure, taken

from previous studies conducted based on the SATBIM concept [54], is applied to further optimise the size of the model without reducing the accuracy of the solution.

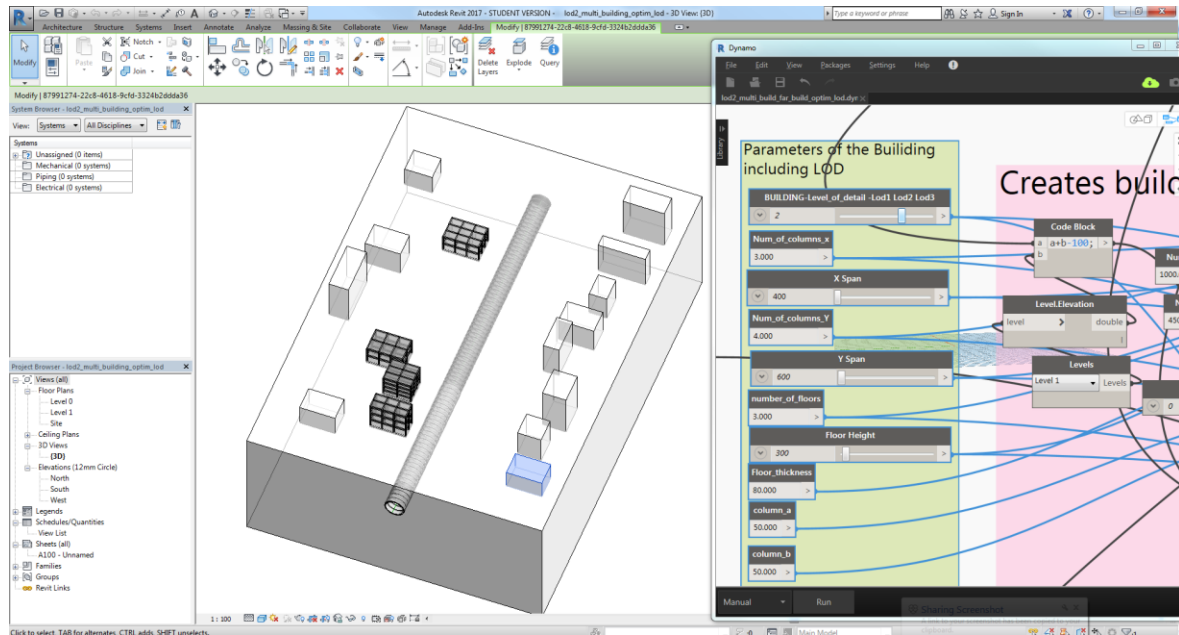


Figure 17: Parametric information model for a 200 m long tunnel section in Revit and Dynamo used for the generation of a large-scale simulation. Selection of the optimal LoD of the building in Dynamo user interface.

In a first simulation all buildings included in the BIM model of the investigated tunnel section are modelled with the highest LoD (see Figure 18a), while in a second numerical analysis, only buildings having a high sensitivity w.r.t. the LoD are modelled with high accuracy, while the rest is modelled with LoD 2, which significantly reduces the size of the problem (see Figure 18b). In both models, LoD 2 is selected for the representation of the tunnel lining structure and the TBM. This model accounts for the shield as a deformable body moving through the soil and interacting with the ground through surface-to-surface contact. The tunnel advance is modelled by means of de-activation of soil elements and installation of the lining rings and grouting elements. Tunnelling-induced deformations are controlled by applying the face support pressure and the grouting pressure at the tunnel face and in the steering gap, respectively. The elasto-plastic Mohr Coulomb model with associative flow rule is used as the constitutive relation between effective stresses and strains in the fully saturated soil. The groundwater level is assumed at the surface. The tunnel is constructed with 80 lining rings of 2.5m length and 10m radius are excavated under 17.5m of soil overburden.

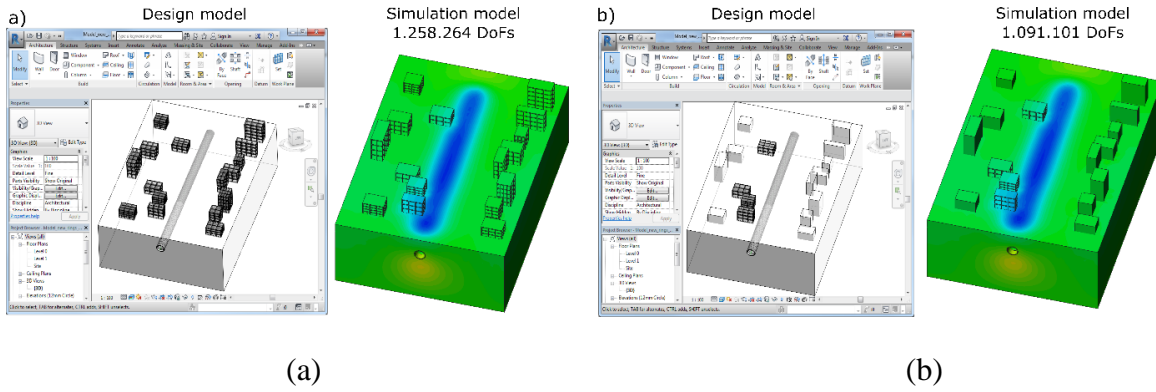


Figure 18: Information (design) and simulation model for a more than 200m long tunnel section used for the generation of a numerical simulation and results of FE simulation generated using “SATBIM-Modeller” for a) Model 1: highest LoD for representation of the infrastructure and b) Model 2: optimised LoD for representation of the infrastructure.

Considering a spatial discretization of all components (soil, lining, TBM and buildings) the models are finally described with 1,258,264 and 1,091,101 Degrees of Freedom (DoFs) for Model 1- high (LoD3) and Model 2- optimised (LoD2 and LoD3) representation of buildings, respectively. Selecting the optimal LoD for the buildings, the model size has been reduced by 17% in terms of number of DoFs, while keeping the accuracy of the numerical solution, as shown in Figure 18a and b. The model size strongly influences the computational costs as shown in Table 2, where the individual as well as the total time for the solution are listed.

Table 2: Runtime for the solution steps of Model 1 and Model 2 from the Figure10.

Computational costs	Model 1 (high LoD)	Model 2 (optimised LoD)
Conditioning time per step[s]	4.2	3.6
Assembly time per step [s]	26.2	19.8
Solve time per step [s]	281.7	244.2
I/O time per step [s]	4.0	3.6
Total time [min]	2916	2410

Although the size of the model and consequently the computational costs differ significantly, the final output of the numerical analysis is identical for Models 1 and 2 as shown in Figure 18. This is due to fact that the complexity of the model is optimised without affecting the important, i.e. the

influencing features of the model w.r.t. the objective of the analysis, which in this case is tunnelling-induced settlements and interaction with existing buildings. Further improvement of the computational efficiency of the SATBIM framework by means of parallelisation is presented in [54].

The SATBIM framework has also been tested on real tunnel data including 3D topology of the ground based on borehole data, 3D tunnel alignment, and building models created based on a City model data, to create and analyse a large tunnel section of approximately 1km length. Figure 19 (a) shows how the SATBIM framework is used for a fully automatic generation of the information model based on the CAD data. The information model was further used for the generation of the simulation models and design assessment of the tunnel construction as illustrated in Figure 19 (b). Initial calculations of a large tunnel section were conducted with a low LoD for the structural components. The evolution of tunnelling-induced displacements and their effects on the existing infrastructure were evaluated as illustrated in Figure 19 (b). Secondly, for the tunnel section, where potential risks on the existing structure have been identified, a more detailed analysis was conducted, adopting higher LoDs for the structural components (lining (LoD 3), buildings (LoD 3) and TBM (LoD 2)) as illustrated in Figure 20.

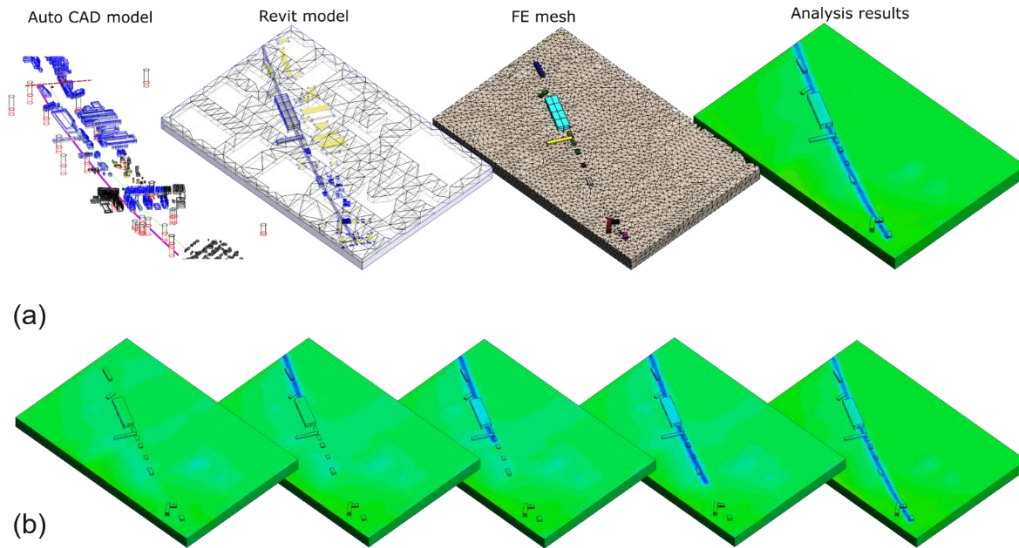


Figure 19. (a) Automated workflow for design and assessment based on project data in SATBIM; (b) development of surface settlements and soil-structure interaction.

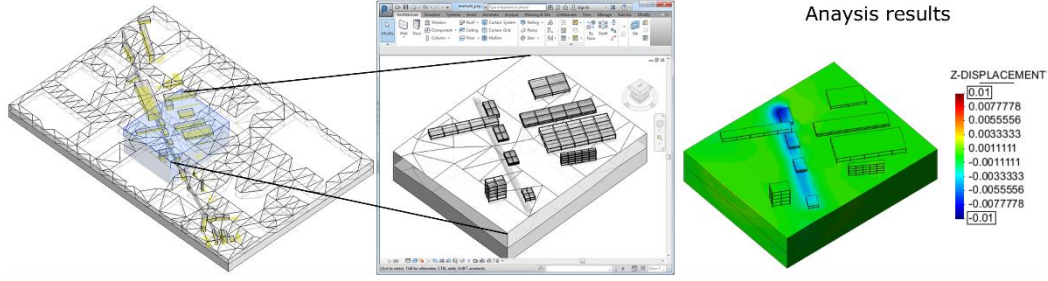


Figure 20. Further evaluation of critical sections considering a higher level of representation for structural components.

3.4 Multi-level IFC representation of a tunnelling project

While Revit only allows the export of one single configuration of the model, where the geometry of the domain models is fixed to a specific LoD, we developed a custom solution to implement the suggest LoD modelling concept. To this end, we implemented the so-called Zero Touch Extension for Dynamo, which uses the IFC Engine DLL Application Interface [55] to integrate multiple LoD configurations into a single IFC file.

As the control of the representation contexts in IFC is limited to the project level, different domain models (buildings, tunnel, TBM and ground) are still exported to separate IFC files. Moreover, each building model of the existing infrastructure should provide different LoDs, resulting in separate IFC files, one per building.

To exemplify the multi-level modelling approach, we present the object diagrams of one of the building models and the tunnel lining model. Figure 21 outlines the object diagram for one of the buildings. The spatial structure is restricted to the level of *IfcBuilding*. Here, the product representation includes three different representations of subtype *IfcShapeModel*. The first, representing geometry for LoD 1, just includes the footprint geometry of the building. The second, representing geometry for LoD 2, includes an extrusion geometry. The last, representing the geometry of LoD 3, includes a multitude of solid geometry elements to constitute the structural model. To link properties to a specific LoD, these representations are assigned to instances of *IfcGeometricRepresentationSubcontext*, whose value of the attribute *UserDefinedTargetView* identifies the LoD, namely either "LOD1", "LOD2" or "LOD3".

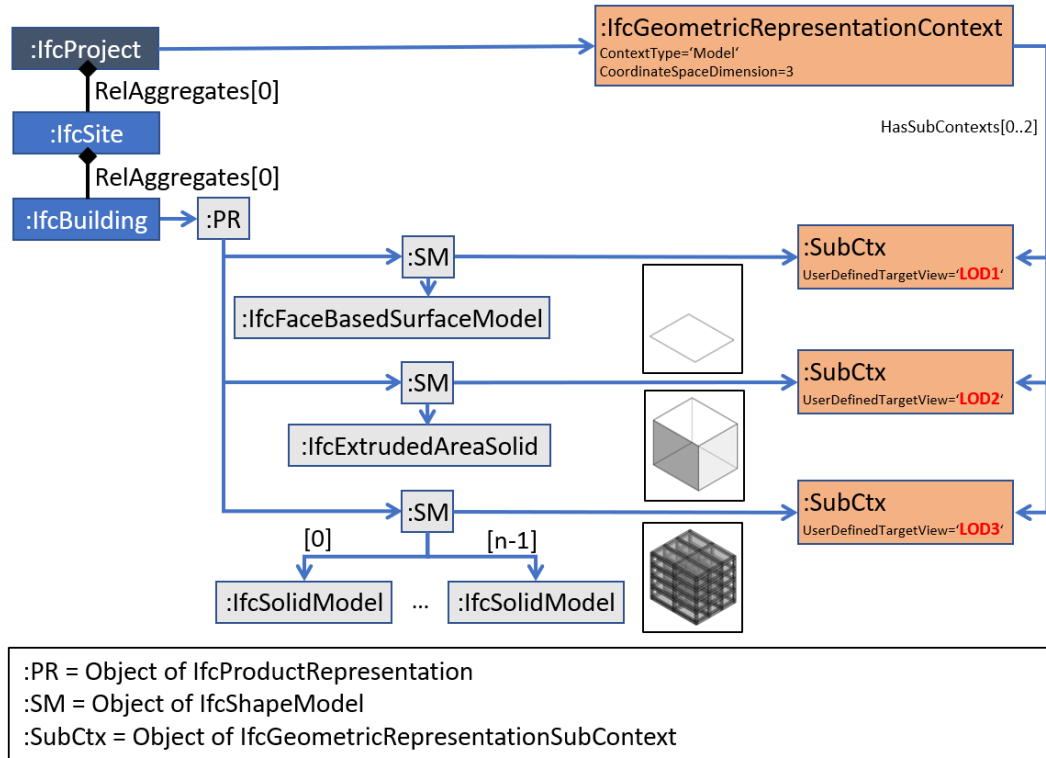


Figure 21: Object diagram demonstrating IFC multi-level modelling of the tunnel lining

While the instantiation of one of the buildings models seems straightforward, the IFC representation of the tunnel lining is more sophisticated. First of all, because the IFC domain actually does not contain any specific classes within the domain of mechanized tunnelling, we utilize an extension previously published in [1], containing the classes *IfcTunnel* and *IfcTunnelRing*, inherited from *IfcSpatialStructureElement* as well as the class *IfcTunnelSegment*, inherited from *IfcElement*. *IfcTunnel* represents the most upper spatial definition of the tunnel lining, similar to the *IfcBuilding* class. It further decomposes into spatial structures for the tunnel rings (*IfcTunnelRing*). The actual physical tunnel segments are finally represented by means of *IfcTunnelSegment*. Figure 22 outlines the object diagram of the tunnel lining.

Since common IFC viewers do not yet distinguish multiple representation contexts, and thus would show all geometries at the same time, we extended the IFC Web-Viewer, which has been introduced in [1], to support such contexts. Figure 23 depicts the configuration of Model 2 (see Fig. 18 b, optimised LoD 2 and LoD 3), which in this case, has not been configured from scratch, but by selecting the proper representation context for each of the exported domain models, e.g. tunnel lining at LoD 2, and building #5 at LoD 3.

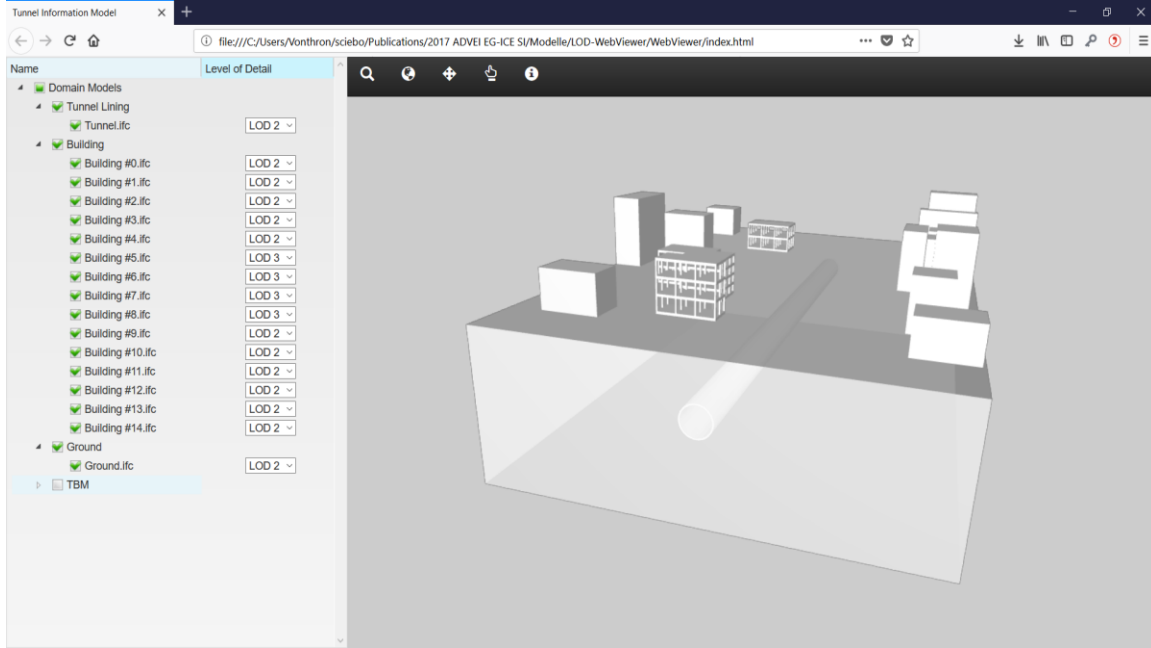


Figure 23: IFC Web-Viewer presenting model geometries from different LoD contexts

4. CONCLUSIONS

Due to increasing urbanisation and mobility there is a need for the efficient and safe design and construction of mechanised tunnels using the latest computer-supported technologies, such as BIM and FE simulations. In this context, existing literature has shown the potential of multi-LoD information models and the need for advanced numerical simulation models. What was missing is the multi-LoD integration of the information and the numerical model.

This paper proposes a novel concept of parametric information modelling for multi-level decision support for mechanised tunnelling projects: SATBIM is an integrated, open-source platform for information modelling, structural analysis and visualisation. Within this platform, industry-standard tools (Autodesk Revit and Dynamo) are employed for the design of the tunnel structure

and the surrounding infrastructure with consideration of LoDs for all system components. Based on the multi-level parametric BIM, multi-level numerical models are developed for each component, considering proper geometric as well as material representation, interfaces and the representation of the construction process. The numerical models are then, fully automatically, instantiated and executed based on the BIM. Finally, the simulation outputs are read back and visualised within Revit.

SATBIM enables efficient design and assessment of design alternatives reducing the modelling efforts and computation time by: (i) minimisation of the efforts needed for model generation; (ii) representation at different LoDs leading to computationally efficient simulations; and (iii) effective visualisation of the simulation results. This modelling and computational efficiency is demonstrated in the numerical example presented in this paper. Applying the optimal LoDs of the components in the information models and automatically generating corresponding numerical simulations, have significantly reduced the computational efforts without affecting the accuracy of the assessment. Further improvement of the computational efficiency can be achieved by using parallelisation strategies or simulation-based meta models [54]. Moreover, the extension for representation of multiple LoD configurations of the TIM components into a single IFC file allows for interoperability of the proposed platform with other BIM tools in a structured and efficient way.

The list below summarises the major contribution of the work presented in this article:

- Concept and implementation of an integrated parametric multi-LoD information and numerical model for mechanised tunnelling that consistently links the corresponding LoD descriptions in both the information and the numerical worlds.
- Software framework that assists the:
 - semi-automated parametric generation of multi-LoD information models
 - automated generation and analysis of a specific-LoD numerical model
- Concept and implementation of a multi-LoD tunnel information model using the Industry Foundation Classes and their functionalities for relations modelling (LoD for the semantics of physical building elements) and for geometric representation contexts (LoD for the geometry of those elements)

The current framework employs FE analysis for the design assessment, and it is well-known that for high accuracy of the numerical solution, a fine discretisation of the FE mesh is required. Therefore, in order to achieve high accuracy of the solution at low computational costs, we aim to integrate Iso-Geometric Analysis (IGA) and make a direct use of the B-rep geometries generated in the BIM for the definition of numerical models. This concept has been proven as successful for

the tunnel lining component [56], and in the future development of our framework, we will work toward integration of design and IGA for the other tunnel components addressed in this study. Another limitation of the current state of development of the framework is the numerical representation of structures at the highest LoD, which at the moment is restricted to geometrical models of the structural frame using linear elastic material models. For more realistic representation of structures and the structural damage induced by tunnelling, our future work will involve development and implementation of damage models, as well as improvements in modelling of details such as connections between the structural elements. The SATBIM toolkit is made available as open source software together with technical report, and benchmark examples deposited in the Github repository: <https://github.com/satbim>.

ACKNOWLEDGEMENTS

The authors gratefully acknowledge the financial support by the European Union's Horizon 2020 research and innovation programme under the Marie Skłodowska-Curie grant agreement No 702874 and the German Research Foundation (DFG) within the subproject D1 of the Collaborative Research Center SFB 837 "Interaction Modeling in Mechanised Tunnelling".

REFERENCES

- [1] C. Koch, A. Vonthron and M. König, “A tunnel information modelling framework to support management, simulations and visualisations in mechanised tunnelling projects,” *Automation in Construction*, vol. 83, pp. 78-90, 2017.
- [2] A. Borrmann, M. Flurl, J. Jubierre, R.-P. Mundani and E. Rank, “Synchronous collaborative tunnel design based on consistency preserving multi-scale models,” *Advanced Engineering Informatics*, vol. 28, no. 4, pp. 499-517, 2014.
- [3] H. Lai and X. Deng, “Interoperability analysis of IFC-based data exchange between heterogeneous BIM software,” *Journal of Civil Engineering and Management*, vol. 24, no. 7, pp. 537-555, 2018.
- [4] S. Lee and B. Kim, “IFC Extension for Road Structures and Digital Modeling,” *Procedia Engineering*, vol. 14, p. 1037–1042, 2011.
- [5] Y. Ji, A. Borrmann, J. Beetz and M. Obergrösser, “Exchange of Parametric Bridge Models Using a Neutral Data Format,” *Journal of Computing in Civil Engineering*, vol. 27, no. 6, pp. 593-606, 2013.
- [6] D. Rebolj, A. Tibaut, N. Cus-Babic, A. Magdic and P. Podbrenznik, “Development and application of a road product model,” *Automation in Construction*, vol. 17, no. 6, p. 719–728, 2008.
- [7] N. Yabuki, T. Aruga and H. Furuya, “Development and application of a product model for shield tunnels,” in *Proc. of the 30th Intl. Symposium on Automation and Robotics in Construction*, Montreal, 2013.
- [8] A. Borrmann, T. Kolbe, A. Donaubaier, H. Steuer, J. Jubierre and M. Flurl, “Multi-scale geometric-semantic modeling of shield tunnels for GIS and BIM applications,” *Computer-Aided Civil and Infrastructure Engineering*, vol. 30, no. 4, p. 263–281, 2015.
- [9] J. Abualdenien and A. Borrmann, “A meta-model approach for formal specification and consistent management of multi-LOD building models,” *Advanced Engineering Informatics*, vol. 40, pp. 135 -153, 2019.
- [10] A. (. I. o. Architects), “AIA contract document G202–2013, building information modeling protocol form,” AIA, Washington DC, 2013.
- [11] BIMForum, “Level of development specification guide,” 2013.
- [12] G. Meschke, J. Ninic, J. Stascheit and A. Alsahly, “Parallelized computational modeling of pile-soil interactions in mechanized tunneling,” *Engineering Structures*, vol. 47, pp. 35-44, 2013.
- [13] N. Do, D. Dias, P. Oreste and D.-M. I., “Three-dimensional numerical simulation for mechanized tunnelling in soft ground: the influence of the joint pattern,” *Acta Geotechnica*, vol. 9, no. 4, pp. 673-694, 2014.
- [14] J. Ninic and G. Meschke, “Model update and real-time steering of tunnel boring machines using simulation-based meta models,” *Tunnelling and Underground Space Technology*, vol. 45, pp. 138-152, 2015.
- [15] N. Nawari and M. Kuenstle, *Building Information Modeling: Framework for Structural Design*, CRC Press, 2015.
- [16] L. Svoboda, J. Novak, L. Kurilla and J. Zeman, “A framework for integrated design of algorithmic architectural forms,” *Advances in Engineering Software*, vol. 72, pp. 109 - 118, 2014.

- [17] M. Breitenberger, A. Apostolatos, B. Philipp, R. Wuechner and K. Bletzinger, "Analysis in computer aided design: Nonlinear isogeometric B-Rep analysis of shell structures," *Computer Methods in Applied Mechanics and Engineering*, vol. 284, pp. 401-457, 2015.
- [18] M. Rafiq and I. MacLeod, "Automatic structural component definition from a spatial geometry model," *Engineering Structures*, vol. 10, no. 1, pp. 37-40, 1988.
- [19] S. Boonstra, K. van der Blom, H. Hofmeyer, M. T. Emmerich, J. van Schijndel and P. de Wilde, "Toolbox for super-structured and super-structure free multi-disciplinary building spatial design optimisation," *Advanced Engineering Informatics*, vol. 36, pp. 86-100, 2018.
- [20] G. Meschke, S. Freitag, A. Alsahly, J. Ninic, S. S. and C. Koch, "Numerical Simulation in Mechanized Tunneling in Urban Environments in the Framework of a Tunnel Information Model," *Bauingenieur*, vol. 89, no. 11, pp. 457-466, 2014.
- [21] J. Ninic, S. Freitag and G. Meschke, "A hybrid finite element and surrogate modelling approach for simulation and monitoring supported TBM steering," *Tunnelling and Underground Space Technology*, vol. 63, pp. 12-28, 2017.
- [22] A. Alsahly, V. Gall, A. Marwan, J. Ninic, G. Meschke, A. Vonthron and K. M., "From Building Information Modeling to Real time Simulation in Mechanized tunneling," in *Proceedings of the World Tunneling Congress 2016*, San Francisco, 2016.
- [23] J. Amann, A. Borrmann, F. Hegemann, J. Jubierre, M. Flurl, C. Koch and M. Koenig, "A refined product model for shield tunnels based on a generalized approach for alignment representation," in *Proc. of the 1st International Conference on Civil and Building Engineering Informatics*, 2013.
- [24] J. Ninić and C. Koch, "Parametric multi-level tunnel modelling for design support and numerical analysis," in *EURO:TUN 2017 - IV International Conference on Computational Methods in Tunneling and Subsurface Engineering*, Innsbruck, Austria, 2017.
- [25] AUTODESK, "Autodesk Revit," 2017. [Online]. Available: <http://www.autodesk.co.uk/products/revit-family/>.
- [26] D. Toll, H. Zhu, A. Osman, W. Coombs, X. Li and M. Rouainia, "Information Technology in Geo-Engineering," in *Proc. of the 2nd International Conference on Information Technology in Geo-Engineering*, 2014.
- [27] D. Aldiss, M. Blac, D. Entwisle, D. Page and R. Terrington, "Benefits of a 3D geological model for major tunnelling works: An example from Farringdon, east-central London, UK," *Quarterly Journal of Engineering Geology and Hydrogeology*, vol. 45, no. 4, pp. 405-414, 2012.
- [28] F. Zobl and R. Marschallinger, "Subsurface geo building information modelling GeoBIM," *Geoinformatics*, vol. 8, no. 11, pp. 40-43, 2008.
- [29] O. Arnau and C. Molins, "Three dimensional structural response of segmental tunnel linings," *Engineering Structures*, vol. 44, no. 0, pp. 210-221, 2012.
- [30] S. Teachavorasinskun and T. Chub-Uppakarn, "Influence of segmental joints on tunnel lining," *Tunnelling and Underground Space Technology*, vol. 25, no. 4, pp. 490-494, 2010.
- [31] J. Burland and C. Wroth, "Settlement of buildings and associated damage," in *Proc. of the Conference on Settlement of Structures*, 1975.
- [32] A. B. Vesic, "Beams on Elastic Subgrade and the Winkler's Hypothesis," in *Proceedings of 5th International Conference of Soil Mechanics*, 1963.
- [33] D. Kolymbas, *Geotechnik - Tunnelbau und Tunnelmechanik*, Springer, 1998.

- [34] F. Nagel and G. Meschke, "An elasto-plastic three phase model for partially saturated soil for the finite element simulation of compressed air support in tunnelling," *International Journal for Numerical and Analytical Methods in Geomechanics*, vol. 34, pp. 605-625, 2010.
- [35] A. Alsahly, J. Stascheit and G. Meschke, "Advanced finite element modeling of excavation and advancement processes in mechanized tunneling," *Advances in Engineering Software*, vol. 100, pp. 198-214, 2016.
- [36] H. Yu, "CASM: a unified state parameter model for clay and sand," *International Journal for Numerical and Analytical Methods in Geomechanics*, vol. 48, pp. 773-778, 1998.
- [37] B. Maidl, M. Herrenknecht, U. Maidl and G. Wehrmeyer, *Mechanised Shield Tunnelling*, Ernst und Sohn, 2012.
- [38] N.-A. Do, D. Dias, P. Oreste and I. Djeran-Maigre, "Three-dimensional numerical simulation for mechanized tunnelling in soft ground: the influence of the joint pattern," *Acta Geotechnica*, vol. 9, no. 4, pp. 673 - 694, 2014.
- [39] T. Kasper and G. Meschke, "A 3D finite element model for TBM tunneling in soft ground," *International Journal for Numerical and Analytical*, vol. 28, pp. 1441-1460, 2004.
- [40] F. Nagel, J. Stascheit and G. Meschke, "Numerical simulation of interactions between the shield supported tunnel construction process and the response of soft, water saturated soils," *International Journal of Geomechanics (ASCE)*, vol. 12, no. 6, pp. 689-696, 2011.
- [41] A. Lamborghini, L. Rodriguez and R. Castellanza, "Development and validation of a 3D numerical model for TBM-EPB mechanised excavations," *Computers and Geotechnics*, vol. 40, pp. 97-113, 2012.
- [42] N.-A. Do, D. Dias, P. Oreste and I. Djeran-Maigre, "2D tunnel numerical investigation: The influence of the simplified excavation method on," *Geotechnical and Geological Engineering*, vol. 32, no. 1, pp. 43-58, 2014.
- [43] G. Meschke, "Consideration of aging of shotcrete in the context of a 3D viscoplastic material model," *International Journal for Numerical*, vol. 39, pp. 3123-3143, 1996.
- [44] T. Kasper and G. Meschke, "On the influence of face pressure, grouting pressure and TBM design in soft ground tunnelling," *Tunnelling and Underground Space Technology*, vol. 21, no. 2, pp. 160-171, 2006.
- [45] V. Founta, J. Ninic, A. Whittle, G. Meschke and J. Stascheit, "Numerical simulation of ground movements due to EPB tunnelling in clay," in *Prof. of the 3rd International Conference on Computational Methods in Tunneling and Subsurface Engineering (EURO:TUN 2013)*, Bochum, 2013.
- [46] F. Nagel and G. Meschke, "Grout and bentonite flow around a TBM: Numerical simulations addressing its impact on surface settlements," *Tunnelling*, vol. 26, pp. 445-452, 2011.
- [47] T. Laursen, *Computational Contact and Impact Mechanics*, Berlin-Heidelberg: Springer, 2002.
- [48] J. Waeytens, B. Rosić, P.-E. Charbonnel, E. Merliot, D. Siegert, X. Chapeleau, R. Vidal, V. le Corvec and L.-M. Cottineau, "Model updating techniques for damage detection in concrete beam using optical fiber strain measurement device," *Engineering Structures*, vol. 129, pp. 2-10, 2016.
- [49] S. Schindler and P. Mark, "Evaluation of building stiffness in the risk-assessment of structures affected by settlements," in *Proceedings of Third International Conference on Computational Methods in Tunneling and Subsurface Engineering*, Bochum, 2013.
- [50] M. Venugopal, C. Eastman, R. Sacks and J. Teizer, "Semantics of model views for information exchanges using the industry foundation class schema," *Advanced Engineering Informatics*, vol. 26, no. 2, pp. 411-428, 2012.

- [51] A. Melendo, A. Coll, M. Pasenau, E. Escolano and A. Monros, “GiD: the personal pre- and postprocessor,” 2017. [Online]. Available: <http://www.gidhome.com/>. [Accessed Januar 2018].
- [52] P. Dadvand and R. Rossi, “Kratos Multi-physics,” International Center for Numerical Methods in Engineering (CIMNE), 2017. [Online]. Available: <http://www.cimne.com/kratos/>. [Accessed Januar 2018].
- [53] J. Ninic, C. Koch and J. Stascheit, “An integrated platform for design and numerical analysis of shield tunnelling processes on different levels of detail,” *Advances in Engineering Software*, vol. 112, pp. 165-179, 2017.
- [54] J. Ninic, H. Bui, C. Koch and G. Meschke, “Computationally Efficient Simulation in Urban Mechanized Tunneling Based on Multilevel BIM Models,” *Journal of Computing in Civil Engineering*, vol. 33, no. 3, p. 04019007, 2019.
- [55] RDF, “IFC Engine,” 2017. [Online]. Available: <http://www.ifcbrowser.com/>. [Accessed 15 November 2017].
- [56] J. Ninic, H. Bui and M. G., “Parametric Design and Isogeometric Analysis of Tunnel Linings within the Building Information Modelling Framework,” in *EG-ICE 2019 Workshop on Intelligent Computing in Engineering*, Leuven, Belgium, 2019.